(2)

IDA PAPER P-2395

CALCULATION OF REENTRY-VEHICLE TEMPERATURE HISTORY

Reinald G. Finke

September 1990

INSTITUTE FOR DEFENSE ANALYSES
1801 N. Beauregard Street, Alexandria, Virginia 22311-1772

IDA Log No. HQ 90-35501

DEFINITIONS

IDA publishes the following documents to report the results of its work.

Reports

Reports are the most authoritative and most carefully considered products IDA publishes. They normally embody results of major projects which (a) have a direct bearing on decisions affecting major programs, (b) address issues of significant concern to the Executive Branch, the Congress and/or the public, or (c) address issues that have significant economic implications. IDA Reports are reviewed by outside panels of experts to ensure their high quality and relevance to the problems studied, and they are released by the President of IDA.

Group Reports

Group Reports record the findings and results of IDA established working groups and panels composed of senior individuals addressing major issues which otherwise would be the subject of an IDA Report. IDA Group Reports are reviewed by the senior individuals responsible for the project and others as selected by IDA to ensure their high quality and relevance to the problems studied, and are released by the President of IDA.

Papers

Papers, also authoritative and carefully considered products of IDA, address studies that are narrower in scope than those covered in Reports. IDA Papers are reviewed to ensure that they meet the high standards expected of refereed papers in professional journals or formal Agency reports.

Documents

IDA Documents are used for the convenience of the sponsors or the analysts (a) to record substantive work done in quick reaction studies, (b) to record the proceedings of conferences and meetings, (c) to make available preliminary and tentative results of analyses, (d) to record data developed in the course of an investigation, or (e) to forward information that is essentially unanalyzed and unevaluated. The review of IDA Documents is suited to their content and intended use.

The work reported in this document was conducted under contract MDA 903 89 C 0003 for the Department of Defense. The publication of this IDA document does not indicate endorsement by the Department of Defense, nor should the contents be construed as reflecting the official position of that Agency.

This Paper has been reviewed by IDA to assure that it meets high standards of thoroughness, objectivity, and appropriate analytical methodology and that the results, conclusions and recommendations are properly supported by the material presented.

REPORT DOCUMENTATION PAGE

Form Approved
OMB No. 0704-0188

1. AGENCY USE ONLY *(Leave blank)*	2. REPORT DATE	3. REPORT TYPE AND DATES COVERED
	September 1990	Final--July to September 1990

4. TITLE AND SUBTITLE

Calculation of Reentry-Vehicle Temperature History

5. FUNDING NUMBERS

C - MDA 903 89 C 0003

T - T-R2-597.12

6. AUTHOR(S)

Reinald G. Finke

7. PERFORMING ORGANIZATION NAME(S) AND ADDRESS(ES)

Institute for Defense Analyses
1801 N. Beauregard St.
Alexandria, VA 22311-1772

8. PERFORMING ORGANIZATION REPORT NUMBER

IDA Paper P-2395

9. SPONSORING/MONITORING AGENCY NAME(S) AND ADDRESS(ES)

SDIO/ENA
The Pentagon
Room 1E149
Washington, DC 20301-7100

10. SPONSORING/MONITORING AGENCY REPORT NUMBER

11. SUPPLEMENTARY NOTES

12a. DISTRIBUTION/AVAILABILITY STATEMENT

Approved for public release; distribution unlimited.

12b. DISTRIBUTION CODE

13. ABSTRACT ***(Maximum 200 words)***

A procedure has been set up to calculate the transient temperature distribution on the surface of a reentry vehicle (RV), with simulation of aerodynamic heating in the free-molecule, transition, and laminar (continuum) flow regimes, one-dimensional transient heat conduction into the heat shield, and reradiation.

The procedure is exercised to determine the altitude dependence of the surface temperature at various points on a particular RV configuration for an example ballistic trajectory for a range of emissivities.

14. SUBJECT TERMS	15. NUMBER OF PAGES
Reentry Vehicle, Aerodynamic Heating, Laminar Convection, Free-Molecule Heating, Bridging, Transient Heat-Conduction, Temperature Distribution, Temperature History, Emissivity	28
	16. PRICE CODE

17. SECURITY CLASSIFICATION OF REPORT	18. SECURITY CLASSIFICATION OF THIS PAGE	19. SECURITY CLASSIFICATION OF ABSTRACT	20. LIMITATION OF ABSTRACT
UNCLASSIFIED	UNCLASSIFIED	UNCLASSIFIED	SAR

IDA PAPER P-2395

CALCULATION OF REENTRY-VEHICLE TEMPERATURE HISTORY

Reinald G. Finke

September 1990

INSTITUTE FOR DEFENSE ANALYSES
Contract MDA 903 89 C 0003
Task T-R2-597.12

ABSTRACT

A procedure has been set up to calculate the transient temperature distribution on the surface of a reentry vehicle (RV), with simulation of aerodynamic heating in the free-molecule, transition, and laminar (continuum) flow regimes, one-dimensional transient heat conduction into the heat shield, and reradiation.

The procedure is exercised to determine the altitude dependence of the surface temperature at various points on a particular RV configuration for an example ballistic trajectory for a range of emissivities.

CONTENTS

FIGURES

I. INTRODUCTION AND SUMMARY

In support of POET analysis of the detection and acquisition ranges of a two-color sensor on a terminal-based interceptor, a procedure has been set up to calculate the transient temperature distribution on the surface of a reentry vehicle (RV). The example exercise of the procedure provided here is for an RV with a reference ballistic coefficient of about 1500 lb/ft^2 reentering at a reentry angle near 25 deg on a ballistic path with a range of about 10,000 km to impact (a reentry velocity of about 23,150 ft/sec). The inputs to the IDA RANGE trajectory program that were used to characterize the hypothetical RV are the following:

Cone half angle = 10 deg,

Ratio of hemisphere cross-sectional area to reference area = 0.041,

Ratio of base area to reference area = 1.00,

Ratio of surface area to reference area = 5.76,

Mass = 750 lb, and

Reference area = 4.55 ft^2.

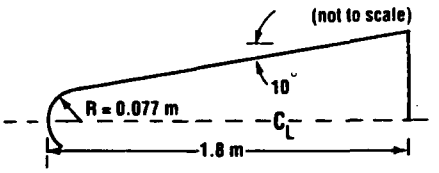

These numbers are consistent with a nose radius of about 3 in. (0.077 m) and an overall length of about 5.9 ft (1.8 m). The reference ballistic coefficient is in effect defined using the hypersonic inviscid drag coefficient, i.e., that for velocities above about Mach 10 where the base drag coefficient has diminished to negligible values and for altitudes below about 200 kft where the skin-friction drag coefficient has diminished to negligible values (IDA, 1969). At lower Mach numbers and at higher altitudes, the overall drag coefficient generally increases above, and the ballistic coefficient decreases below, the reference value. The reentry angle is defined as the path angle measured from the horizontal at an altitude of 400 kft.

The results of the example calculations, considering free-molecule or continuum-flow (laminar) aerodynamic heating in the appropriate altitude regimes (with "bridging" in the transition between them), reradiation with an emissivity of 0.25, and one-dimensional transient heat conduction into a glass-fiber-phenolic heat shield, indicate that the stagnation

point on the nose reaches the "ablation" temperature, arbitrarily taken as 2000 K, at an altitude of about 260 kft, and that the surface of all of the conical body passes through a temperature of 1000 K at an altitude of about 250 kft and reaches the "ablation" temperature at an altitude of about 200 kft.

II. ANALYSIS

The principal questions addressed by the analysis were the following:

(1) What governs the input heating at different points on the RV?

(2) What governs the thermal response of the RV surface?

Considerations involved in (1) include the determination of (a) the functional dependences, and altitude regions of applicability, of free-molecule heating and laminar convection at the stagnation point, (b) the flight conditions on the particular reentry trajectory as a function of time, and (c) the heating distribution at points other than the stagnation point on a hemisphere-cone body.

Considerations involved in (2) include determinations of (a) the transient thermal response, i.e., time-dependent heat conduction into the heat-shield material, (b) typical physical properties of a glass-fiber-phenolic ablative heat shield, and (c) the dependence of surface temperature on emissivity (a discretionary, not inherent, property of the surface).

The heat transfer rate at the stagnation point in the free-molecule flow regime, q_{FM}, is given in Gilbert and Scala, 1965, as

$$q_{FM} = \frac{a}{2} \rho_\infty V_\infty^3 \left(1 + \frac{1}{2\sqrt{\pi}\, S_\infty} \right) \text{ft-lb/(ft}^2 \text{ sec)}$$

where

a = accommodation coefficient (taken as 1.0)

ρ_∞ = local free-stream atmospheric density (slug/ft^3)

V_∞ = vehicle flight velocity with respect to the local atmosphere (ft/sec)

$S_\infty = M_\infty \sqrt{\gamma/2}$

M_∞ = vehicle flight Mach number

γ = ratio of the specific heats of air.

For Mach numbers of 16 or greater (typical of the heating regime of interest for reentry-vehicle detection and tracking), the molecular-speed correction term $\left(1/\left(2\sqrt{\pi}\ S_\infty\right)\right)$ has a value less than two percent.

Ignoring the molecular-speed correction term, and changing the units to more convenient (for comparison with laminar heat-transfer below) values, the formula for free-molecule heating at the stagnation point becomes

$$q_{FM} = 1.528 \times 10^6 \left(\frac{\rho_\infty}{\rho_0}\right)\left(\frac{V_\infty}{10^4}\right)^3 \text{ Btu/(ft}^2\text{sec)} \quad ,$$

where ρ_0 is the atmospheric density at sea level.

The here-adopted empirical correlation* for the hypersonic laminar ("continuum") heat-transfer rate at the stagnation point, q_L, is (per IDA, 1966, p. 22, leaving out for the moment a factor depending on surface temperature which is close to 1 for most cases of interest)

$$q_L = \frac{865}{\sqrt{R_n}} \sqrt{\frac{\rho_\infty}{\rho_0}} \left(\frac{V_\infty}{10^4}\right)^{3.15} \text{ Btu/(ft}^2\text{ sec)} \quad ,$$

where R_n is the hemispherical-nose radius in feet. The missing correction factor, involving the flight velocity and a value of the yet-to-be-determined surface ("wall") temperature T_w, is

$$\left[\frac{V_\infty^2 - 6.75 \times 10^6\ (T_w/289)}{V_\infty^2 - 6.75 \times 10^6}\right] \quad ,$$

where T_w is in degrees Kelvin. This factor will be included later in the transient analysis, in which a value of the wall temperature becomes available.

The above two formulas for the stagnation-point heating in the free-molecule regime (q_{FM}, varying as ρ_∞) and the laminar flow regime (q_L, varying as $\sqrt{\rho_\infty}$) yield the same value at a "crossover" altitude, defined by a "crossover" atmospheric density ρ_c given by

$$\rho_c/\rho_0 = \left(2.0230 \times 10^{-8}/R_n\right) V_\infty^{0.3} \quad .$$

---

* This correlation is in numerical agreement with that of Detra, Kemp, and Riddell as validated with data in Perini, 1975.

The crossover altitude for an R_n of 3 in. and a V_∞ of 23,000 ft/sec (typical of the example ballistic missile trajectory) is about 303 kft for the 1962 Model Atmosphere used in RANGE.

In the transition regime between free-molecule and laminar heating the effective heating $\bar{q}$ is assumed to vary in a smooth way, without a sudden discontinuity in slope, and is typically faired between the two regimes with a "bridging" function (see Matting, 1971). In this analysis we adopt a general bridging relation that preferentially weights the lesser of the two values according to

$$\bar{q} = \left(\frac{1}{q_{FM}^n} + \frac{1}{q_L^n} \right)^{-1/n} = q_L \frac{q_{FM}/q_L}{\left[1 + (q_{FM}/q_L)^n \right]^{1/n}} \quad ,$$

where

$$q_{FM}/q_L = \sqrt{\rho_\infty/\rho_c} \quad .$$

A plot of the transition behavior of $\bar{q}/q_c$ (where q_c is the value from either heat-transfer relation when ρ_∞ equals ρ_c) as a function of ρ_∞/ρ_c for this general bridging relation, for values of n of 1 and 2, is shown in Figure 1, with transition using the Matting (op. cit.) bridging function included for comparison. A value of 2 for the exponent n is chosen in subsequent analysis here; some other value (e.g., 1.6) could be easily substituted when better data (than those included in Matting, 1971) become available.

If the convective heat-transfer rate $\bar{q}$ is expressed as an equivalent radiation rate of a surface with an emissivity e = 1 and no thermal inertia (or no heat conduction), an equivalent radiative-equilibrium surface temperature, T_{eq}, can be used to characterize the aerodynamic heating. The following formula to give this T_{eq} (in degrees Kelvin) from local flight conditions was derived from the above equations for $\bar{q}$ (with n = 2), and has been incorporated in the RANGE trajectory program:

$$T_{eq} = 1000 \left[173.4 \sqrt{(\rho_\infty/\rho_0)(\rho_\infty/\rho_c)/(1+\rho_\infty/\rho_c)} \; (V_\infty/10^4)^{3.15}/\sqrt{R_n} \; \right]^{1/4} \quad .$$

The output value of this T_{eq} from RANGE is used to describe the aerodynamic heating, as σT_{eq}^4 [$\sigma = 5.672 \times 10^{-12}$ watt/(cm^2 K^4)], in the subsequent transient heat-conduction analysis, in conjunction with the wall-temperature correction factor that uses the corresponding output value of flight velocity from RANGE. The aerodynamic heating, in terms of this "inertialess" radiative-equilibrium stagnation-point temperature (consistent

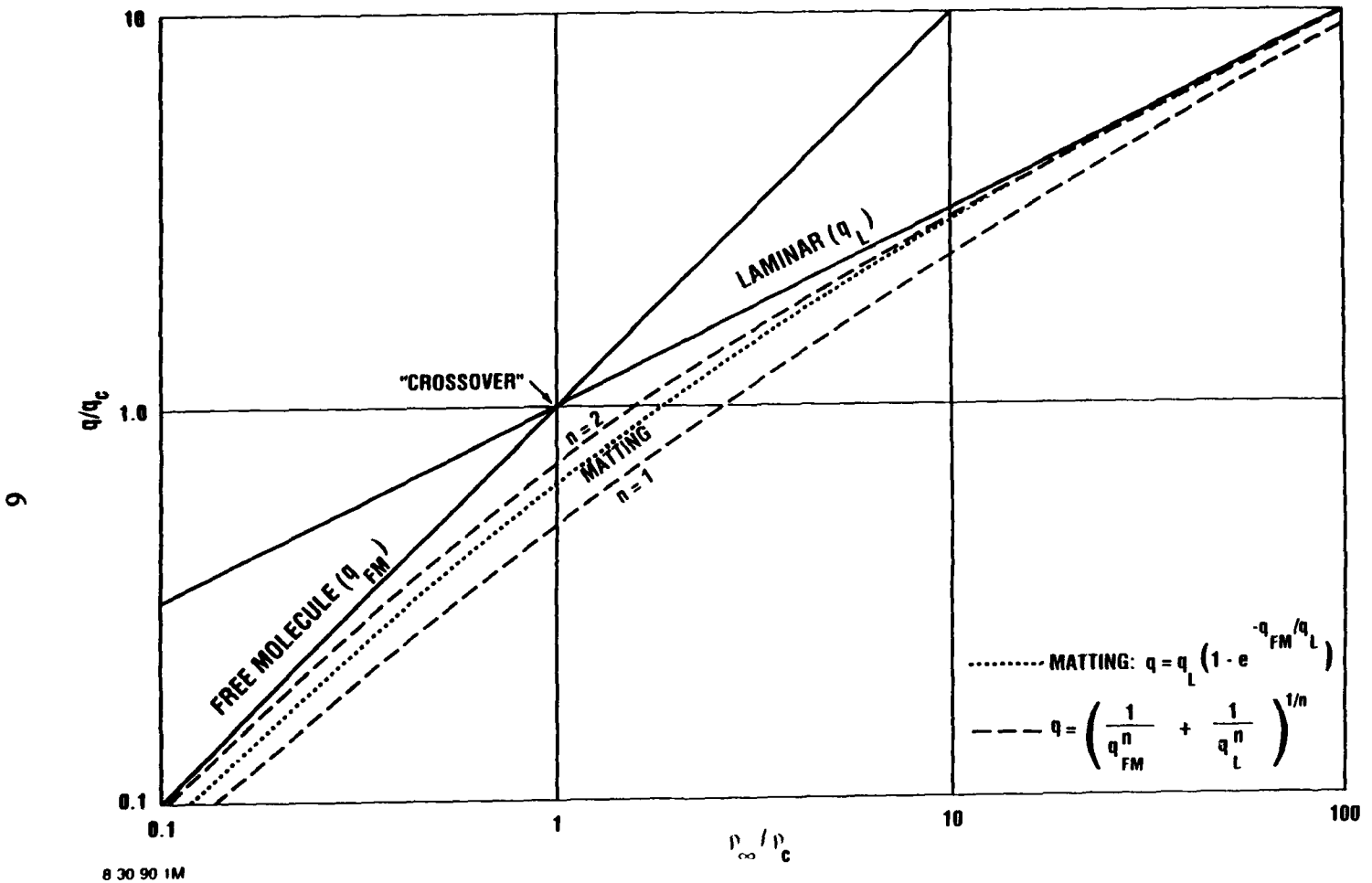

Figure 1. Comparison of "Bridging" Relations for the Transition from Free Molecule to Laminar Heating (Velocity Constant; No Wall Temperature Correction)

with an assumed wall temperature of 289 K) for the desired reentry trajectory is shown in Figure 2. The flight velocity for the wall-temperature correction factor (incorporated in the transient analysis where the wall temperature is determined) varies only between extremes of 22,960 and 23,440 ft/sec in the descent from 547 kft to 127 kft in the example reentry trajectory.

At points other than the stagnation point on a hemispherical nose, the heat transfer rate q drops off with angle around the hemisphere from the stagnation point as shown in Figure 3. (The influence on heat transfer at a downstream point by the evolution of gases from an upstream point into the boundary layer is not considered.) The heat transfer on the conical surface is assumed to be constant at the value at the shoulder, based on the constancy of pressure on a conical surface (NAVWEPS, 1961, p. 154) and the one-to-one correspondence of heat transfer with pressure (Detra and Hidalgo, 1961, Fig. 1 therein). From the curve in Figure 3, the relative heat-transfer rate q/q_s (where q_s equals the $\bar{q}$ above) as a function of distance s from the stagnation point for our 0.077-m-radius-hemisphere/10-deg-cone body is given in the following table:

s/R, deg	q/qs	s, m	
0	1.0	0.000	(stagnation point)
20	0.93	0.027	
40	0.72	0.054	
60	0.45	0.081	
80	0.22	0.108-1.858	(shoulder and conical surface)

The transient behavior of the surface temperature is computed by the TRIDE program (IDA, 1974) from the input heating-rate history derived from the RANGE inertialess radiative-equilibrium stagnation-point temperatures (Fig. 2). The TRIDE computer program (reproduced in the Appendix) is a numerical solution of the one-dimensional* time-dependent heat-conduction equation

$$\frac{\partial T}{\partial t} = \frac{k}{c\rho} \frac{\partial^2 T}{\partial x^2}$$

---

* The adequacy at one-dimensional versus two-dimensional analysis will be addressed by comparing the magnitudes of the gradients in the two directions, normal to the surface and parallel with the surface. If the gradient (i.e., heat flow) along the surface is small in comparison with the gradient into the surface, its neglect in the heat flow analysis is acceptable.

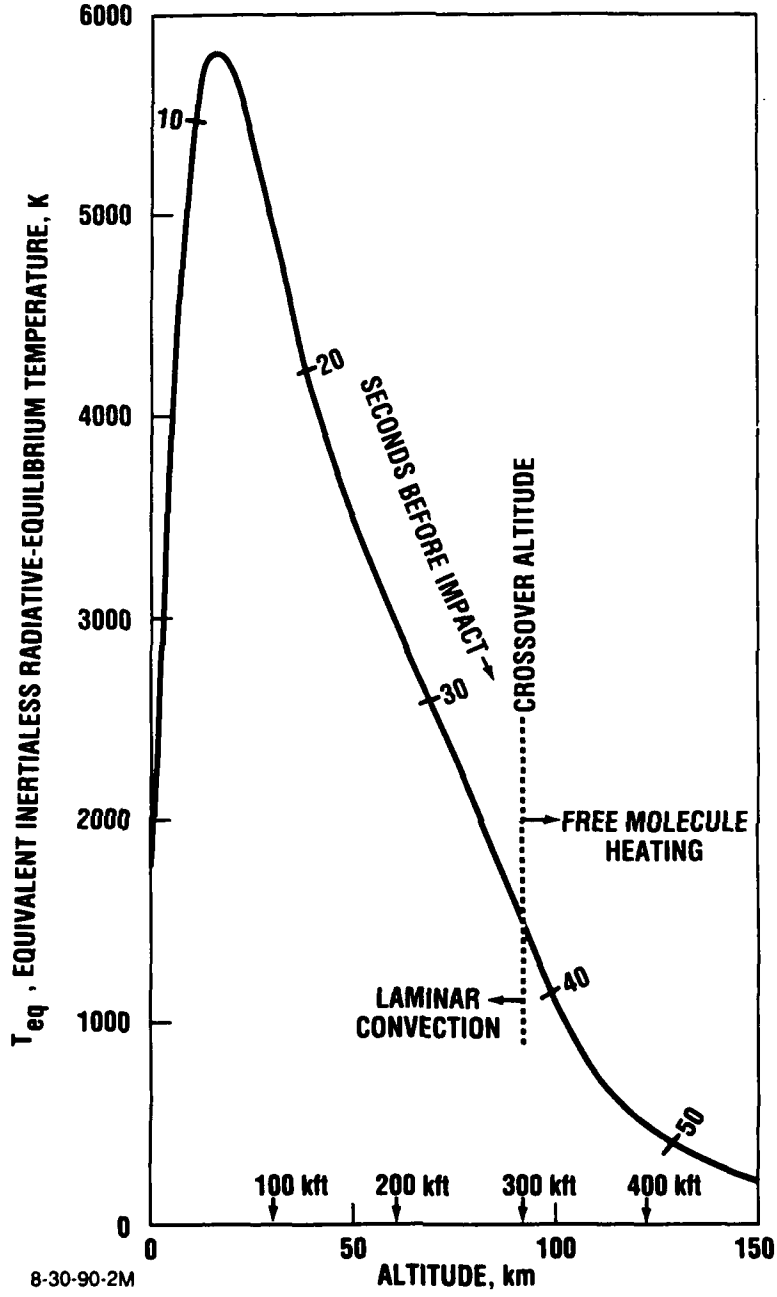

Figure 2. Aerodynamic Heating Rate at Stagnation Point (R_n = 0.077 m) in Terms of Equivalent "Inertialess" Radiative-Equilibrium Temperature (for T_w = 289 K) (for ICBM Reentry Vehicle: β = 1500 lb/ft^2; γ = − 24.8°; R_{impact} = 10,020 km)

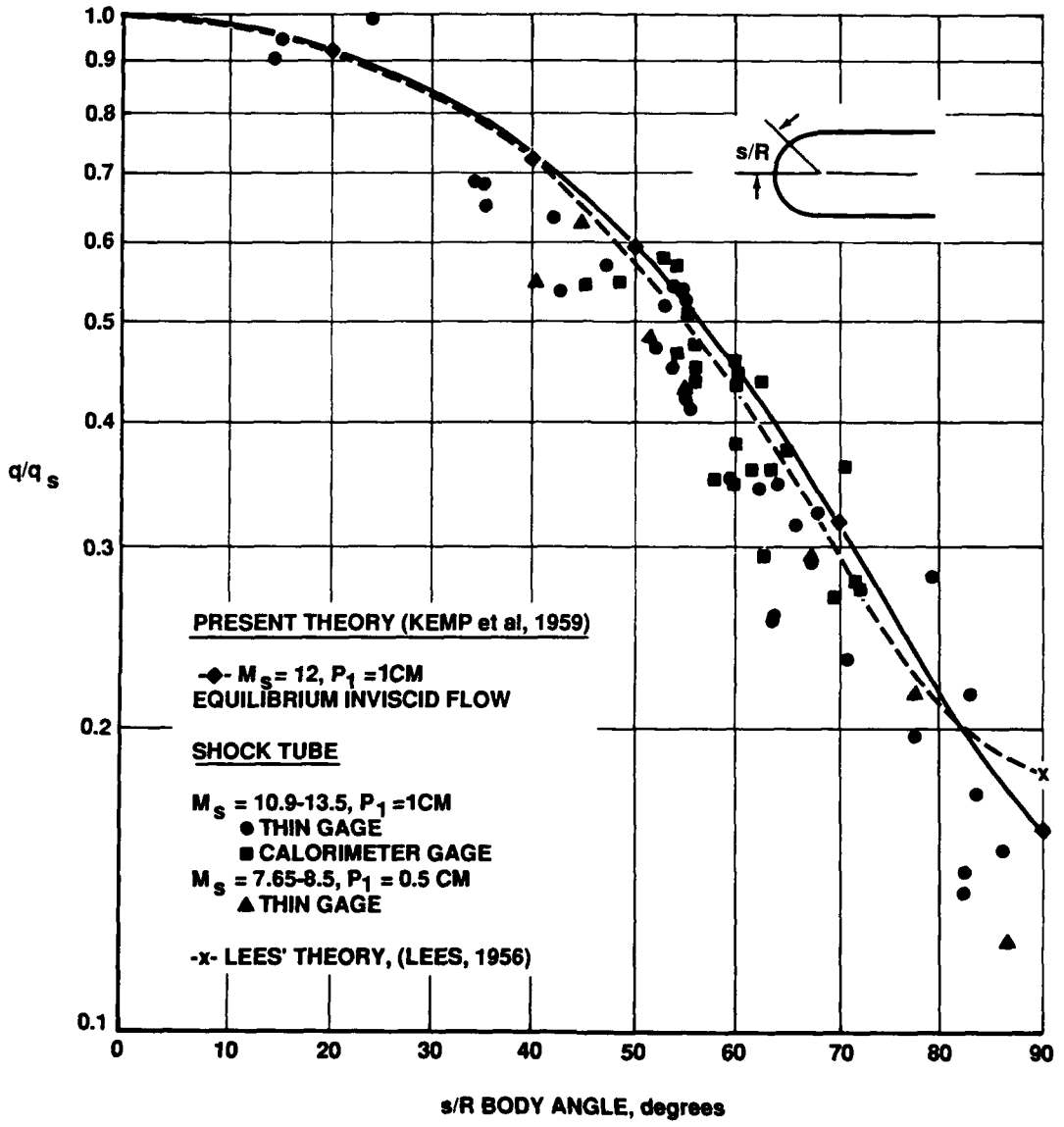

Figure 3. Heat-Transfer Distribution on Hemisphere Cylinder (From Kemp et al., 1959; see reference for definition of parameters)

using the implicit-differencing technique (see Appendix). The calculation treats an infinite plate of finite thickness heated on one side and insulated on the other. At each time step (one-second interval) the aerodynamic heating, in terms of equivalent radiation at the inertialess temperature T_{eq} corrected with a surface ("wall") temperature factor, is absorbed, some is reradiated according to the surface temperature T_w and the emissivity e, and the remainder is conducted inward to raise T_w and the internal temperature, according to the boundary condition

$$k\frac{\partial T}{\partial x} = -\sigma T_{eq}^4 \left(\frac{V_\infty^2 - 6.75 \times 10^6 (T_w/289)}{V_\infty^2 - 6.75 \times 10^6} \right) + e\sigma T_w^4 \quad .$$

The T_w used in the reradiation term and in the correction factor is extrapolated to the present instant by means of a cubic extrapolation from the four previous values. The temperature within the thickness of the plate is computed at 10 points, the centers of 10 equal subdivisions, e.g.,

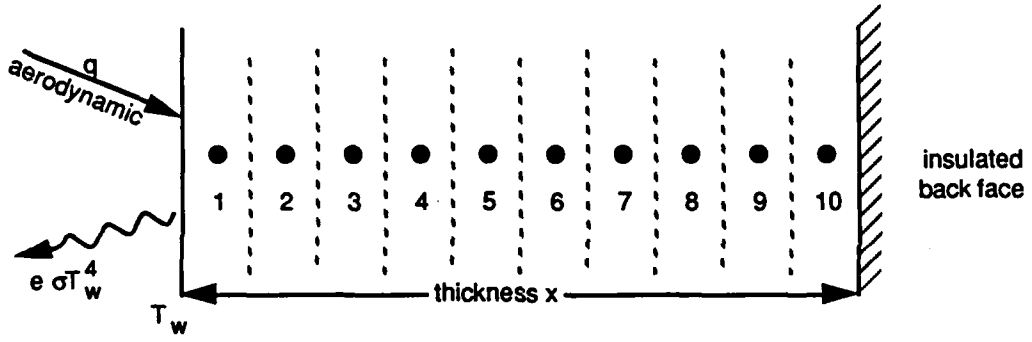

The thickness chosen for the calculations here is small enough to provide adequate detail in the temperature contour but large enough to include all the material that may experience a temperature rise during the period of interest. The thermal conductivity k, heat capacity c, density ρ, and emissivity e are constants in the calculation. When the material in the first cell reaches the "ablation" temperature, taken arbitrarily as an even 2000 K, the calculation is stopped.

The physical properties for "glass-fiber phenolic" for purposes of this introductory exercise were taken from the *Handbook of Materials Science*, Vol. III, p. 34, and are the following (temperature dependences were ignored):

k = 0.20 Btu/(hr ft F) = 0.000826 cal/(cm sec C),

c = 0.30 Btu/(lb F) = 0.30 cal/(gm C), and

$\rho = 1.825$ gm/cm^3.

For these values and the experienced heating rates, a thickness of 0.5 cm is found to be appropriate; i.e., the back-face temperature at 0.5-cm depth starts to rise at about the time that the front-face temperature reaches the assumed temperature of ablation.

The emissivity is a parameter of choice by the RV designer depending on his selection of an external coating, and is varied in the family of calculations over the range of 0.25 to 1.0.

III. CALCULATIONAL PROCEDURE

As a recapitulation of the analysis described above, the calculational procedure is made up of the following steps:

1. Convert flight-vehicle characteristics to RANGE inputs.
2. Run RANGE to provide the stagnation-point aerodynamic heating, expressed as an equivalent inertialess radiative-equilibrium temperature, and the flight velocity as functions of time and altitude.
3. Select appropriate values of conductivity, heat capacity, density, and thickness of the vehicle's heat shield. (The material properties can be temperature dependent.)
4. Insert heat-shield properties and second-by-second values of the stagnation-point aerodynamic heating, i.e., the inertialess radiative-equilibrium temperature, and flight velocity in TRIDE.
5. Select values of the ratio to the stagnation-point heating for the heating at desired points on the vehicle.
6. Run TRIDE to give the time dependence of the temperature profile within the wall of the heat shield for the heat-transfer ratios at the desired points. Adjust the thickness of the heat shield so that the temperature of the back face would just start to rise at the end of the period of interest, and return to step 4, above.

IV. EXAMPLE RESULTS

The temperature history on the RV surface at the stagnation point and on the shoulder and conical surface, calculated by the procedure outlined above, is plotted as a function of altitude and time in Figure 4. For a surface emissivity of 0.25, the temperature at the stagnation point passes through 1000 K at an altitude of about 290 kft and reaches the "ablation" temperature (taken as 2000 K) at about 260 kft; the temperature at the shoulder and on all the conical surface passes through 1000 K at about 250 kft and reaches the "ablation" temperature at about 200 kft.

The temperature distribution on the RV surface at altitudes 5 seconds apart is shown in Figure 5 for an emissivity of 0.25. The contour at the crossover between free-molecule heating and laminar convection is indicated by the dotted curve. The steepest slopes of the contours along the surface (just before the shoulder on the hemisphere) are only 2 to 3 percent of the internal temperature gradients just within the surface at the shoulder, shown in Figure 6; two-dimensional calculations should show little change from the one-dimensional results.

The dependence of surface temperature on emissivity for the baseline RV and trajectory at four altitudes is given by the following table (in degrees Kelvin):

emissivity =	0.25	0.50	0.75	1.00
stagnation-point temp at 295.8 kft (90.17 km)	886	876	866	857
stagnation-point temp at 266.3 kft (81.18 km)	1857	1725	1626	1542
conical-surface temp at 246.6 kft (75.18 km)	1021	1001	984	969
conical-surface temp at 207.1 kft (63.13 km)	1890	1746	1654	1592

The fairly weak dependence of surface temperature on emissivity indicates that reradiation plays a smaller part than conduction in dispersing the aerodynamic heating from the RV surface, even with the low conductivity of glass-fiber phenolic.

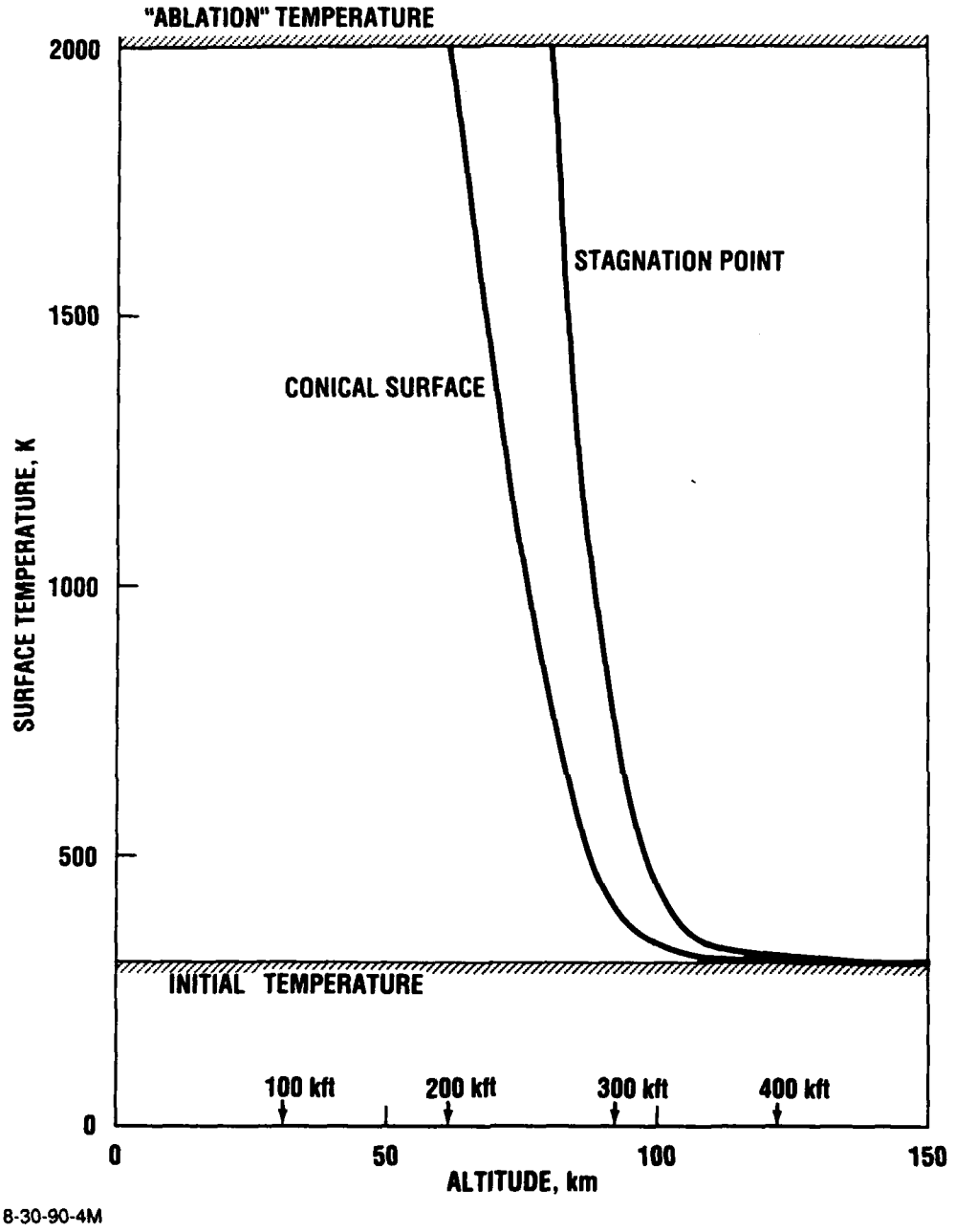

Figure 4. Temperature History on ICBM RV Surface at Two Points (aerodynamic heating; one-dimensional heat conduction in glass-fiber phenolic; emissivity = 0.25) $\beta \sim 1500$ lb/ft^2 (nose radius = 0.077m); $\gamma = -24.8°$; $R_{impact} = 10{,}020$ km

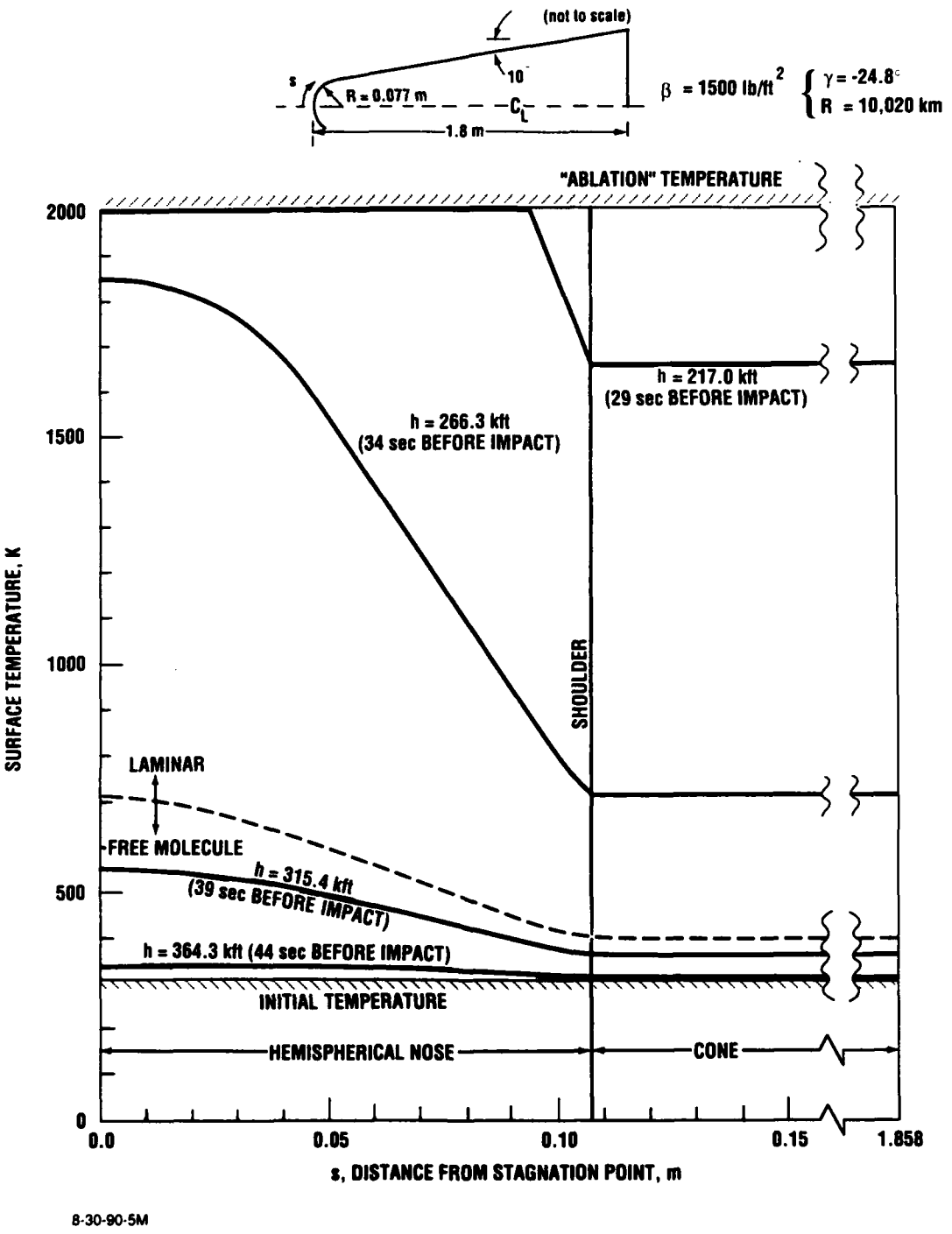

Figure 5. Temperature Distribution on ICBM RV Surface at Different Altitudes (aerodynamic heating; one-dimensional heat conduction in glass-fiber phenolic; emissivity = 0.25)

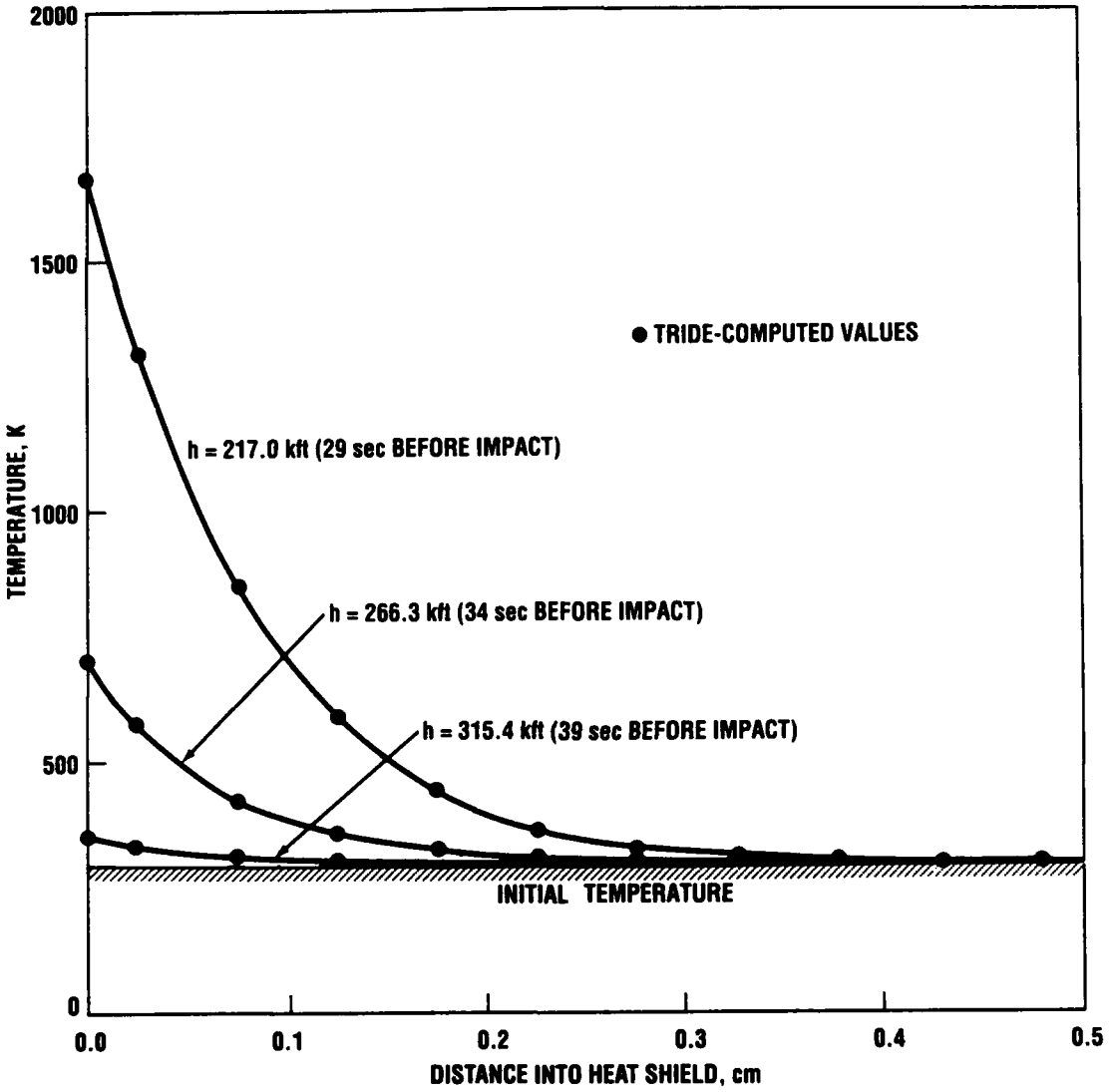

Figure 6. Temperature Profile Within Heat Shield at Hemisphere-Cone Shoulder at Different Altitudes for the Example Reentry Trajectory for the Example RV Configuration With a Glass-Fiber Phenolic Heat Shield; emissivity = 0.25

V. OBSERVATIONS

Inclusion of the effects of transient heat conduction produces a dependence of total emittance on emissivity; total emittance would be independent of emissivity if conduction were ignored.

The values for the total gray-body emittance ($e\sigma T^4$) for the temperatures in the table in the EXAMPLE RESULTS are

emissivity =	0.25	0.50	0.75	1.00
Total Emittance (watt/cm^2) at				
stagnation point at 295.8 kft	0.87	1.67	2.39	3.06
stagnation point at 266.3 kft	16.86	25.11	29.74	32.07
conical surface at 246.6 kft	1.54	2.85	3.99	5.00
conical surface at 207.1 kft	18.09	26.36	31.84	36.43

As emissivity is reduced, the total emittance (the integral over the gray-body spectrum) decreases, even though the temperature increases. (If conduction had been ignored, $e\sigma T^4$ would have been independent of e and would have been just σT_{eq}^4, i.e., equal to the aerodynamic heat-transfer rate.) The energy received by a broad-band detector, such as a bolometer, would decrease by a factor of two or more as the emissivity is reduced from 1.0 to 0.25. For a detector sensing in a wavelength band beyond the wavelength of greatest spectral emittance, λ_{max} (given by Wien's displacement law: $\lambda_{max}\, T \approx 0.3$ cm K; e.g., $\lambda_{max} \approx 3$ μm for T = 1000 K), the ratio of the energy in that band to the total energy would decrease as the temperature is increased, so the spectral emittance (watt/(cm^{2}K)) would decrease even faster than the total emittance as the emissivity is reduced.

On the basis of this argument, an RV designer desiring to minimize the detectability of his RV would choose a surface coating with the lowest practicable emissivity up to the temperature at which the surface starts to break down and evolve gases.

REFERENCES

Detra and Hidalgo, 1961 — Detra, R.W. and H. Hidalgo, "Generalized Heat Transfer Formulas and Graphs for Nose Cone Re-Entry Into the Atmosphere," *ARS Journal*, Vol. 31, No. 3, March 1961.

Gilbert and Scala, 1965 — Gilbert, L.M. and S.M. Scala, "Free Molecule Heat Transfer in the Ionosphere," in Singer, S.F., *Interactions of Space Vehicles with an Ionized Atmosphere*, Pergamon Press, 1965.

IDA, 1966 — Finke, R.G., Chairman, *Technologies and Economics of Reusable Space Launch Vehicles*, IDA Report R-114, Vol. II, February 1966.

IDA, 1969 — Finke, R.G., *Reentry Vehicle Dispersion due to Atmospheric Variations*, IDA Paper P-506, August 1969.

IDA, 1974 — Finke, R.G., *Initial A-22 Calculations of Space-Laser Damage Threshold*, IDA Memorandum, April 5, 1974.

Kemp et al., 1959 — Kemp, N.H., P.H. Rose and R.W. Detra, "Laminar Heat Transfer Around Blunt Bodies in Dissociated Air," *Journal of the Aero/Space Sciences*, July 1959.

Lees, 1956 — Lees, L., "Laminar Heat Transfer Over Blunt-Nosed Bodies at Hypersonic Flight Speeds," *Jet Propulsion*, Vol. 26, No. 4, April 1956.

Matting, 1971 — Matting, F.W., "Approximate Bridging Relations in the Transitional Regime Between Continuum and Free-Molecule Flow," *Journal of Spacecraft*, Vol. 8, No. 1, January 1971, pp. 35-40.

NAVWEPS, 1961 — NAVWEPS Report 1488, *Handbook of Supersonic Aerodynamics*, Vol. 3, Section 8, "Bodies of Revolution," Bureau of Naval Weapons, October 1961.

Perini, 1975 — Perini, L.L., "Compilation and Correlation of Stagnation Convective Heating Rates on Spherical Bodies," *Journal of Spacecraft*, March 1975.

Richtmyer and Morton, 1967 — Richtmyer, R.D. and K.W. Morton, "Difference Methods in Initial Value Problems," Vol. 4 in *Interscience Tracts in Pure and Applied Mathematics*, Wiley, 1967.

APPENDIX

TRANSIENT HEAT CONDUCTION

IMPLICIT DIFFERENCING TECHNIQUE

(adapted from Richtmyer and Morton, 1967)

Diffusion Equation

(1) $$\frac{\partial T}{\partial t} = \frac{k}{c\rho}\frac{\partial^2 T}{\partial x^2}$$

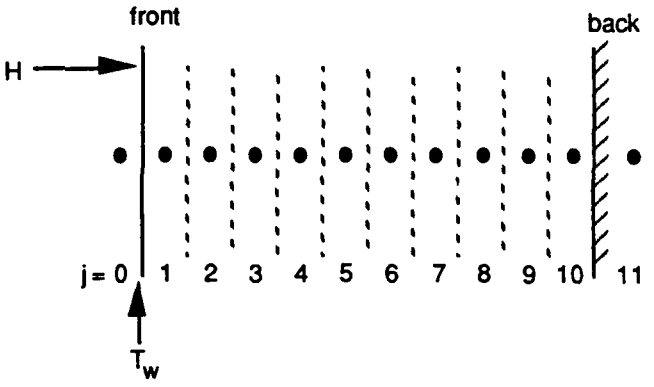

Equivalent Difference Equation

$$\frac{T_j^{n+1} - T_j^n}{\Delta t} = \frac{k}{c\rho}\frac{1}{2(\Delta x)^2}\left[\left(T_{j+1}^n - 2T_j^n + T_{j-1}^n\right) + \left(T_{j+1}^{n+1} - 2T_j^{n+1} + T_{j-1}^{n+1}\right)\right]$$

or

(2) $$T_j^{n+1} = T_j^n + \frac{k}{c\rho}\frac{\Delta t}{2(\Delta x)^2}\left[\left(T_{j+1}^n - 2T_j^n + T_{j-1}^n\right) + \left(T_{j+1}^{n+1} - 2T_j^{n+1} + T_{j-1}^{n+1}\right)\right]$$

$$a \qquad -\psi_j^n$$

so the new temperatures, at the next (n + 1st) time step in terms of values at the nth time step, are

(3) $$a\ T_{j+1}^{n+1} - (2a+1)\ T_j^{n+1} + a\ T_{j-1}^{n+1} = \psi_j^n \quad .$$

If we assume there exists a recursion formula for T_{j+1} such as

(4) $$\boxed{T_j^{n+1} = c_j^n\ T_{j-1}^{n+1} + d_j^n}$$ (compute T in ascending j)

then (3) becomes

$$a\ T_{j+1}^{n+1} - (2a+1)\ T_j^{n+1} + \frac{a}{c_j^n}\left(T_j^{n+1} - d_j^n\right) = \psi_j^n$$

or

$$T_{j+1}^{n+1} = \underbrace{\frac{1}{a}\left(2a+1 - \frac{a}{c_j^n}\right)}_{c_{j+1}^n} T_j^{n+1} + \underbrace{\left(\frac{\psi_j^n}{a} + \frac{d_j^n}{c_j^n}\right)}_{d_{j+1}^n}$$

so the recursion formulas for c, d are

$$\boxed{\begin{aligned} c_j^n &= a/\left(2a+1 - a c_{j+1}^n\right) \\ d_j^n &= c_j^n\left(a d_{j+1}^n - \psi_j^n\right)/a \end{aligned}} \quad \text{(compute c, d in descending j)}$$

Boundary Conditions

back: $T_{11} = c_{11}\ T_{10} + d_{11} = T_{10}$ (insulated wall at $j = 10\frac{1}{2}$)

$$\rightarrow \boxed{d_{11}^0 = 0\ ;\ c_{11}^0 = 1} \rightarrow c_{10}^0 = a/(a+1)\ ;\ d_{10}^0 = -\psi_{10}^0/a\ \ldots\ldots$$

front: $T_1 - T_0 = \frac{H\Delta x}{k}$ at $j = \frac{1}{2}$ $\rightarrow$ $\boxed{T_1^{n+1} = \frac{c_1^n H\Delta x/k - d_1^n}{c_1^n - 1}}$

$$T_w = (3T_0 + 6T_1 - T_2)/8 \quad \text{(quadratic interpolation)}$$

Verification

The implicit differencing numerical procedure used in the TRIDE program (copy appended) was checked against an analytical solution* to the diffusion equation, for a constant heating rate H, a thickness b, and a diffusivity $D = k/c\rho$, which is

---

* Supplied by Dr. Irvin W. Kay.

$$T(x,t) = T_0 + \frac{H}{k}\left[Dt/b - b/6 + (x-b)^2/(2b) - \frac{2b}{\pi^2}\sum_{n=1}^{\infty}(-1)^n \frac{\cos\frac{n\pi(x-b)}{b}}{n^2} e^{-\frac{Dn^2\pi^2}{b^2}t} \right] .$$

The procedure with a $\Delta x = b/10$ (as above) and a $\Delta t = 0.1$ sec reproduced the values given by the analytical solution to within 1 degree (out of $\lesssim$ 300) at all points at all times. For a $\Delta t = 1$ sec, it became obvious that the temperatures given by the numerical procedure were 0.5 sec behind the analytical solution (with the same ~ 1 deg accuracy); the initial time step is $\Delta t/2$. Changing the Δx to b/100 from $\Delta x = b/10$ for $\Delta t = 1$ sec did not change the wall temperatures by more than 1 degree after the first time step.

```
      PROGRAM TRIDE                !RV-HEATING W/WALL TEMP CORR 8/15/90
      DIMENSION T(12), C(12), D(12), P(12)
      DIMENSION TEQ(44), ALT(44), VEL(44)
      DATA TEQ/130.,142.,154.,168.,183.,200.,218.,237.,259.,282., 308.,
     & 335..366..399.,435.,475.,525.,576.,636.,711., 795.,889.,999.,
     & 1127..1264..1414.,1575.,1729.,1883..2039., 2186.,2324..2459.,
     & 2592.,2724.,2856.,2992.,3135.,3281.,3436., 3601.,3788.,3993.,
     & 4214./
      DATA ALT/547.5,537.9,528.4,518.8,509.2,499.6,490.0,480.4,470.8,
     & 461.1, 451.5,441.8,432.2,422.5,412.8,403.1,393.4,383.7,374.0,
     & 364.3, 354.5,344.8,335.0,325.2,315.4,305.6,295.8,286.0,276.2,
     & 266.3, 256.5.246.6,236.8,226.9,217.0,207.1,197.2,187.3,177.4,
     & 167.5, 157.5,147.6,137.7,127.7/
      DATA VEL/22960.,22973.,22986.,22998.,23011.,23024.,23037.,23050.,
     & 23062.,23075., 23088.,23101.,23114.,23127.,23140.,23153.,23166.,
     & 23179.,23192.,23205., 23218.,23231.,23244.,23257.,23270.,23283.,
     & 23296..23310.,23322.,23336., 23348.,23361.,23374.,23386.,23398.,
     & 23409.,23419.,23428.,23435.,23439., 23440.,23434.,23419.,23388./
  102 FORMAT(4X, 3HALT, 5X, 2HTW, 4X, 2HT1, 4X, 2HT2, 4X, 2HT3, 4X,
     &  2HT4, 4X, 2HT5, 4X, 2HT6, 4X, 2HT7, 4X, 2HT8, 4X, 2HT9, 4X,
     &  3HT10)
      PI = 3.1415926536
      SIG = 5.672E-12/4.186
      EM = 0.25
      XK = 0.000826
      CP = 0.3
      RHO = 1.825
      TA = 2000.
      TO = 300.
      X = 0.5
      DT = 1.
      DX = X/10.
  103 FORMAT(2X, 11H INPUT HFAC)
    1 CONTINUE
      TYPE 103
      READ(5,*) HFAC
      IF(HFAC .EQ. 0.) GO TO 99
      TYPE 102
      DO I = 1, 12
        T(I) = TO
      END DO
      TW = TO
      C(12) = 1.
      D(12) = 0.
      DO 10 K = 1, 44
      TWX = TW
      IF(K .EQ. 3) TWX = 2. * TW - TWP
      IF(K .EQ. 4) TWX = 3. * TW - 3. * TWP + TWPP
      IF(K .GT. 4) TWX = 4. * TW - 6. * TWP + 4. * TWPP - TWPPP
      IF(TWX .GE. (TA-50.)) GO TO 1
      TWC = TWX
      Q = SIG * HFAC * (TEQ(K))**4 *
     &  (VEL(K)*VEL(K) - 6.75E6 * TWC/289.)/(VEL(K)*VEL(K) - 6.75E6)
      H = (-Q + EM * SIG * TWX**4) * DX/XK
      DO I = 1, 10
        J = 12 - I
        A = XK * DT/(CP * RHO * 2. * DX * DX)
        P(J) = -(T(J) + A * (T(J+1) - 2. * T(J) + T(J-1)))
        C(J) = A/(2. * A + 1. - A * C(J+1))
        D(J) = C(J) * (A * D(J+1) - P(J))/A
      END DO
      T(2) = (C(2) * H - D(2))/(C(2) - 1.)
      T(1) = (T(2) - D(2))/C(2)
      DO J = 3, 12
        T(J) = C(J) * T(J-1) + D(J)
      END DO
      TWPPP = TWPP
      TWPP = TWP
      TWP = TW
      TW = (3. * T(1) + 6. * T(2) - T(3))/8.
  100 FORMAT(2X, F6.1, 2X, 11(F6.0))
      TYPE 100, ALT(K), TW, (T(M), M = 2, 11)
   10 CONTINUE
      GO TO 1
   99 STOP
      END
```